Light field display using multi-projectors based on splicing algorithm

<u>Kui Ma</u>[*, **], Renjing Pei[*, **], Zheng Geng[*], Zhaoxing Zhang[*]

* School of Computer and Control Engineering, University of Chinese Academy of Sciences, Beijing, China,
** The State Key Laboratory of Management and Control for Complex Systems, Institute of Automation, Chinese Academy of Science, Beijing, China

Keywords: light field, multi-projectors, splitting-splicing

ABSTRACT

We present a light field reconstruction algorithm based on splitting-splicing theory increasing number of viewpoints without increasing the number of projectors, which can adjust the distance of two adjacent view images for higher 3D sensation.

1. INTRODUCTION

Recent advances in light field 3D display technologies facilitate high fidelity 3D scene reconstruction that can be seen without need of any viewing aids, enabling a more realistic reproduction of the true light field distribution of the 3D scene. Many new 3D displays provide true 3D images with smooth motion parallax. Examples of existing multi-projection light field display solutions such as HOLOVIZIO system[1], and other excellent systems[2, 3]. In this article, we apply the light field techniques to improve the performance of a multi-projector 3D display system. Our main contributions in this paper include:

1) In order to reduce the crosstalk[4] and the jumping between viewpoints, we developed a light field reconstruction model for the splicing algorithm to overcome the limit on the number of viewpoints.

2) By our new method, the distance of two adjacent view images can be simply adjusted to human's pupillary distance for a higher 3D sensation.

2. Material and methods

2.1 System Overview

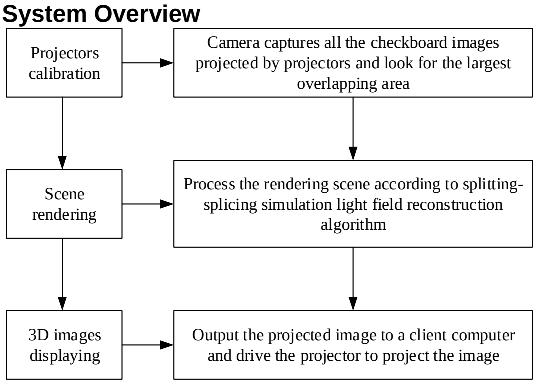

Fig. 1 The overview of our system.

The major hardware components of our naked eye 3D display system consist of a holographic diffuser screen, a multi-projector array and a mirror surface. The light field reconstruction algorithm to obtain the projected image processes the 3D scene content. This image is projected onto the screen by the projector array to form the modulated spatial light field for 3D viewing with naked eyes. Our system is designed as a Horizontal Parallax Only (HPO) system that only offers the horizontal parallax. The overview of our system is given in Fig.1.

2.2 Hardware Components

We designed and constructed a functional experimental system (in Fig. 2) that contains a main control station connecting three client computers to control twenty-nine projectors. The projection light is mirrored to the horizontal holographic diffuser screen

1) Projector: We used twenty-nine DELL MH110 projectors to form a projector array. Each projector offers a WXGA (1,280 by 800) resolution, with 300 lux brightness. The projection distance is 1.61m and the effective display area is 1.11*0.62 m.

2) Holographic diffuser screen: We used a holographic diffuser screen, which made by LUMINIT. It used holographic diffuser technology to create pseudo-random micro-lens structures and gave the light anisotropy property on the screen. The light was shaped by spreading radiation 60^o in horizontal direction, while only 1^o in the vertical direction. The observer can view the complete image in the vertical direction.

3) Mirror: We used a folding mirror to reduce the dimension and to convert the viewing direction of the overall 3D display system. The viewers can look downward to the table-like display screen to see the displayed 3D images. The mirror simply reflects the light from the projector light to the viewers' eyes to view the 3D image. In the following discussion, we discuss our theory, algorithms and design principle without the consideration of the folding mirror's reflection.

Since the diffusing angle δ of the holographic diffuser screen is 1^o, the angle θ interval of the projector is designed 0^o to eliminate the jumping between the adjacent views (in Fig.3). Since the center of the two projectors spaced apart at the angle $\varepsilon = 1^o$ in our system, the refraction of light ray can be ignored. So during the ray path's calibration, we just adjust each projection area on the screen to one region (see details in Sec.4.2). This is in contrast to many existing light field reconstruction algorithms [5] that require complex calibration algorithms to obtain spatial position.

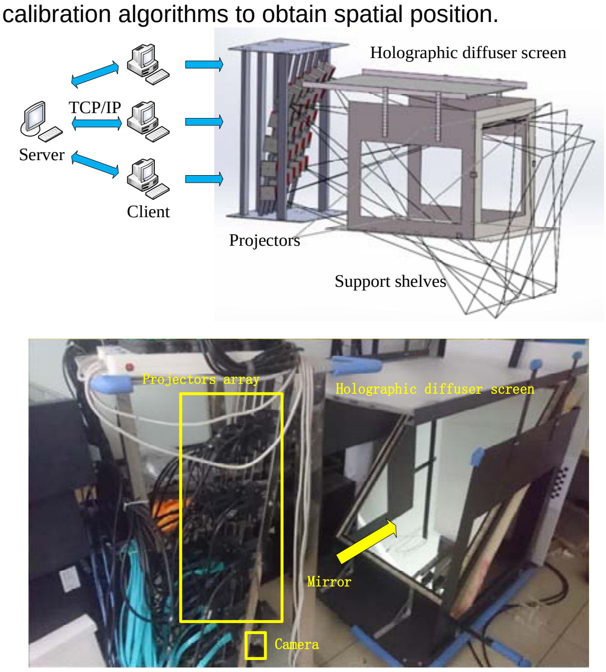

Fig. 2 System structure diagram and the hardware

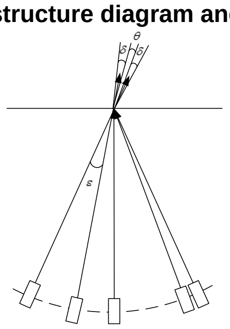

Fig. 3 Diffuser angle and the relative positions among projector units of the projectors

3. Theory and Algorithms

3.1 Rendering Algorithm

The light field reconstruction algorithm is based on the distributed image recombination multi-angle algorithm[6]. The projected images are a set of the rays emitted from the projectors. After image recombination, the image projected by a single projector is not a whole image for viewing. For instance in Fig. 4, point "A" which observed at the viewpoint *View1*, is generated by the light rays emit from the projectors "F" and "H", and point "B" comes from the projectors "E" and "G" when viewed at the viewpoint *View2*.

As analyzed in Sec.3.2, our rendering algorithm starts from the display screen. We focus all projectors to the same screen area (W * H) where each pixel produces a light spot. The system only generates the horizontal parallax, and the screen diffuses all light rays at a considerable angle in the vertical direction. Therefore, we ignore the vertical dimension and only analyzes the algorithm in the horizontal dimension.

Compared with the conventional method, our algorithm doesn't require that the number of viewpoints N_{view} is same as that of the projectors N_{proj}. According the algorithm, although the number of projectors is limited, is feasible to render a great number of viewpoints with high display quality. In our experiments (see details in Sec.4.1 and 4.4), twenty-nine projectors can produce ninety-nine viewpoints and the greater number of viewpoints make the motion parallax smoother.

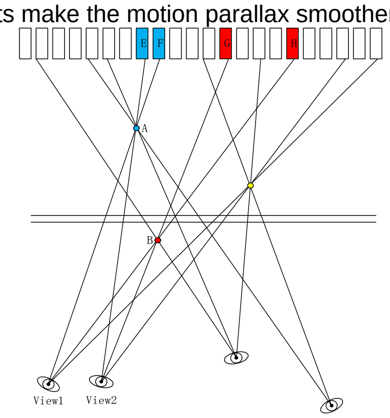

Fig. 4 Light field. The projected module image is not a view of the final 3D image.

In Fig. 5(a), the screen display area is divided equally into N_{view} vertical blocks for processing. In Fig. 5(b), we establish a spatial Cartesian coordinate system orientated at the center of the screen. The projector position $P(x_{p_i}, z_{p_i})$ and a point $S(x_s, 0)$ on the screen determine each ray. In addition, all the rays generate a completely light field as:

$$proj\_Lights = \bigcup_{i=1}^{N_{proj}} \bigcup_{s=1}^{N_{block}} \left[(x_s, 0) - (x_{p_i}, z_{p_i}) \right] \quad i \in each\ projector, s \in each\ block \qquad (1)$$

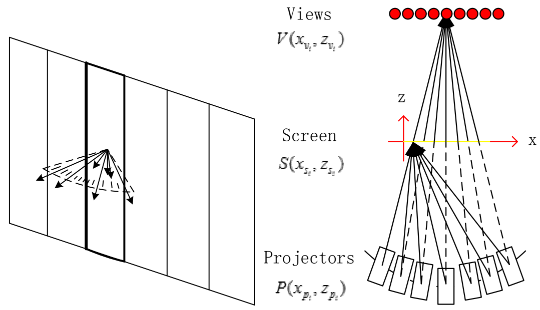

(a) (b)

Fig. 5 (a) shows the area of the block and the projector light emission direction. (b)Split splicing simulation of light field reconstruction algorithm.

In (1), we choose the "N_{view}" points where the most rays aggregated position as the viewpoint, and the number of viewpoints are set to be the number N_{block} of blocks, so $N_{block} = N_{view}$. That is, each block will correspond to a point of view. When the observer looks down onto the screen, N_{proj} different direction lights are injected into the eye upwards. At each viewpoint $V(x_{v_i}, z_{v_i})$, it is possible to see the $(N_{proj} - 1)/2$ blocks on both sides, so that the total number of rays viewed from all viewpoints is

$$view\_Lights = \bigcup_{s=1}^{N_{view}} \bigcup_{i=s-\frac{N_{proj}-1}{2}}^{s+\frac{N_{proj}-1}{2}} \left[(x_s, 0) - \left(x_{v_i}, z_{v_i}\right)\right] \; i \in each\ views, s \in each\ blocks \quad (2)$$

As analyzed above, the number of rays in the set $view\_Lights$ and set $proj\_Lights$ are the same. In our image recombination algorithm, the mapping between the "3D" image of scene and the 2D image projected from projector is produced in the following way:

*I*mage projected on the screen area are segmented into N_{view} blocks. We use a two-dimensional index $Proj[i, j]$ to describe index of projection image and the whole indexes of $Proj$ are equal to the set $proj\_Lights$, where "i" represents the position of the projector, and "j" represents the position of the block in the i^{th} projector image. And $Screen[p, q]$ (the whole indexes of $Screen$ are equal to the set $viewLights$) is the index of the light, where "p" is the location of the block, and "q" presents the block of the light direction index. $View[vp, vb]$ presents the index of view image of the block, where "vp" represents the position of the viewpoint, and "vb" represents the position of the block in the "vp" viewpoint image. $leftRay$ indicates the number of rays of the light on the left side of the viewpoint, and $rightRay$ indicates the number of rays of the light on the right side of the viewpoint; in the viewpoint image, the "vb" block at the "vp" viewpoint is mapped to the projector images.

$$p = \left\lfloor \left[(j-1) * N_{proj} + \left(N_{proj} - i + 1\right)\right] / N_{proj} \right\rfloor \quad (3)$$

$$q = mod\left(\left[(j-1) * N_{proj} + \left(N_{proj} - i + 1\right)\right] / N_{proj}\right) \quad (4)$$

$$leftRay = min\left(N_{proj} - q, p - 1\right) \quad (5)$$

$$rightRay = min(N_{view} - p, q - 1) \quad (6)$$

$$vp = i + \left[j - \left(\left\lfloor N_{proj}/2 \right\rfloor + 1\right)\right] \quad (7)$$

$$vb = \begin{cases} vP - N_{proj}/2 + leftRay & vP > N_{proj}/2 \\ leftRay & vP < N_{proj}/2 \end{cases} \quad (8)$$

When $N_{view} = N_{proj}$, the number of space viewpoints is N_{proj}. This model is similar to the multi-angle model; when $N_{proj} = Width_{image}$, the screen in the horizontal direction of each pixel can produce a view and the model is similar to the whole light field reconstruction model. And the distance of two adjacent view images can be simply adjusted to human's pupillary distance for a higher 3D sensation.

3.2 Projectors Calibration

Factors like the assembly error may cause misalignment of projected images, thus shrinking the overlapping area of all the projected images. As a result, projectors must be precisely aligned to get the largest possible projection overlap area to facilitate the light field reconstruction algorithm.

1) The image of a chessboard with known geometric parameters $X_{ref} = (x_r, y_r)$ is projected onto the screen $X_{world} = (x_w, y_w, y_w)$. We used a CCD camera to collect the chessboard image pattern on the screen and denote it as $X_{camera} = (x_c, y_c)$;
2) We apply image processing techniques to extract the corner locations from the chessboard image captured by the CCD camera. Then, we calculate the checkpoint between the grid and the projection screen image between the single matrix, $X_{world} = H_{ref} * X_{ref}$. After that, the camera checkerboard image corners and the projection screen images between the single matrix is get as: $X_{camera} = H_{cam} * X_{world}$;
3) We can now find the largest overlapping area determined by the corners of the chessboard and make it a rectangular through alignment. The four corners of the rectangular can be obtained as $X_{want} = (x_{cw}, y_{cw})$. The homographic matrices between the corresponding four corners for all the captured images can be calculated as $X_{want} = H_{cam} * X_{camera}$;
4) Finally, we calculate the matrix of each projector from the standard image of the image projected onto the overlapping area.

$$H = H_{ref}^{-1} * H_{cam}^{-1} * H_{want} * H_{cam} * H_{ref} \quad (9)$$

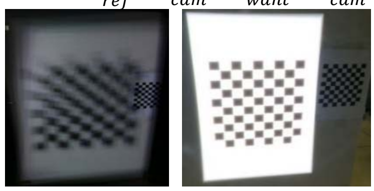

(a) (b)

Fig. 6 Calibration result. The projector (a) does not align the checkerboard image (b) after calibration

4. Experimental Results

4.1 Display Results

Our system uses twenty-nine projectors and segment the number of splicing 99 blocks ($N_{proj} = 29, N_{view} = 99$). Viewing the screen at different positions in the horizontal direction, the observer is able to view the different angle images of the scene. The different position images are as presented in Fig. 7. Besides, we can modify the 3D sensation by simply adjust the parameter N_{view}.

Fig. 7 Different angular display result.

4.2 Display Optimization

We used double layers of holographic diffuser sheers to produce 3D images with smoother transition between viewpoints. We found that using double layers reduces jumping effect between viewpoints. By adapting this hardware modification, we enhanced the 3D display quality and viewing experience, without needing complex software coding and computing resources. When using of the single-layer holographic diffuser screen, due to its horizontal small diffusing angle, the large vertical diffusing angle of the special optical characteristics makes the vertical splitting of the stripes obvious. The diffuser screen into a vertical light bar diffuses the laser beam. Using the CFTOOL toolbox of MATLAB, the intensity distribution of the light bar is analyzed, and any horizontal data of the red channel is fitted, the data distribution is Gaussian model. The result is shown in Fig. 8. Gaussian filter causes fuzzy edge in the image, so we use of double holographic diffuser screens in our system as shown in Fig. 9.

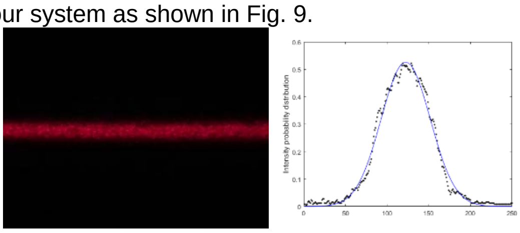

(a) (b)

Fig. 8 (a)The laser is shot through the light bar after the scattering screen. (b)Light intensity distribution and Gaussian fitting results.

(a) (b)

Fig. 9 (a) single-layer diffuser screen display (b) double-layer diffuser screen display

4.3 Similarity Evaluations

After the projection of the reconstructed 3D image, we capture them and compare with the original view image emitted from the projections. In Fig. 10, it records the result by using double-layer diffuser screen with different N. Result is shown in Fig.11.

(a) (b) (c) (d) (e)

Fig. 10 double-layer diffusing screen different N_{view} value effect (a) N_{view} = 49 (b) N_{view} = 99 (c) N_{view} = 149 (d) N_{view} = 199 (e) is not segment

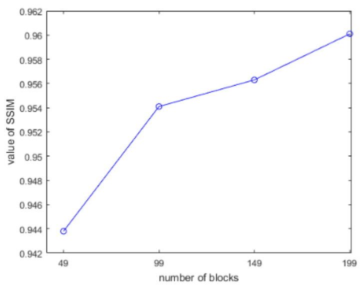

Fig. 11 SSIM result

4.4 3D Perception

When the observer views a 3D image, the left and right eye receive different view images to produce a 3D effect. Different separating blocks number *N* lead to distinctive 3D perception. We test the 3D perception by displaying two letter patterns (e.g. "A" and "B") at two adjacent viewpoints. Then, we record the distance (viewpoint interval) between a clear "A" and "B" at the viewing plane by a moving SLR camera. When the distance smaller than the pupil distance, observer can receive different view images, resulting in high 3D sense.

As shown in the Fig. 12, with the increase of N_{view}, the viewpoint interval decreases. When $N_{view} > 39$, the distance between the two viewpoints is approximately to the pupil distance (0.062m) and the eyes can simultaneously see the clear image "A" and the image "B". When the distance between the two neighboring views is smaller than the pupil distance, the observer will have a stronger 3D sense because of the larger rotation angle between two adjacent viewpoints. Besides, a large N_{view} will reduce the crosstalk effect and in our experimental system, $N_{view} > 49$ is satisfied.

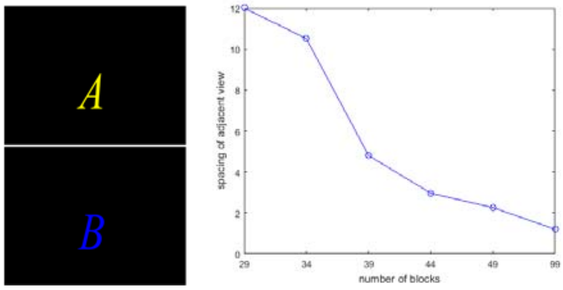

Fig. 12 spacing between adjacent points when separating different blocks

Acknowledgements

This work has been supported by projects of National 863 Program of China (Grant No. 2015AA015905).

REFERENCES

[1] T. Balogh *et al.*, "The Holovizio system–New opportunity offered by 3D displays," in *Proceedings of the TMCE*, 2008, pp. 79-89.

[2] J. H. Lee, J. Park, D. Nam, and S. Y. Choi, "Optimal Projector Configuration Design for 300 ‐ Mpixel Light ‐ Field 3D Display," *Sid Symposium Digest of Technical Papers,* vol. 44, no. 1, pp. 400-403, 2014.

[3] A. V. Jones and M. T. Bolas, "Interpolating vertical parallax for an autostereoscopic three-dimensional projector array," *Journal of Electronic Imaging,* vol. 23, no. 1, p. 011005, 2014.

[4] A. J. Woods, "Crosstalk in stereoscopic displays: a review," *Journal of Electronic Imaging,* vol. 21, no. 4, pp. 040902-040902, 2012.

[5] V. K. Adhikarla, "Rendering and interaction on projection-based light field displays," Pázmány Péter Katolikus Egyetem, 2015.

[6] S. Li, H. Li, and Y. Peng, "Three - Dimensional Display of Stereo Based on Field Stitching," *Chinese Journal of Liquid Crysials and Displays,* no. 04, pp. 601-604, 2010.